

Modeling and Simulation of Incompressible Flow in a Two-Dimensional Domain with Buoyancy Effects

Luiz Gustavo da Silva[1] - silva.luiz_6@posgraduacao.uerj.br
Ygor Ares[3] - ygor.ares@gmail.com
Cristiane Oliveira de Faria[2] - cofaria@ime.uerj.br
Norberto Mangiavacchi[1] - norberto.mangiavacchi@eng.uerj.br
[1]Universidade do Estado do Rio de Janeiro, PPGEM - Rio de Janeiro, RJ, Brazil
[2]Universidade do Estado do Rio de Janeiro, PPG-CCOMP - Rio de Janeiro, RJ, Brazil
[3]Universidade do Estado do Rio de Janeiro, FEN - Rio de Janeiro, RJ, Brazil

Abstract. *This paper presents the direct simulation of the low Reynold number turbulent incompressible flow of a particulate fluid with buoyancy effects in a two-dimensional domain. The simulation variables are velocity, pressure and concentration of particulate. All equations (The Navier-Stokes and transport) used were discretized, in a coupled way, by the Galerkin Finite Element method, using the semi-implicit Theta method for the time approximation, resulting in a single system of non-linear equations for each time step. The computational implementation was performed using the Julia programming language, with the Gridap package for the assembly of the Finite Elements approximation and the solution of the resulting system of equations using Newton's method. The parameters that were used in the simulations to obtain comparisons of results were Reynolds number, Froude number and the magnitude of the settling velocity using three cases. The simulation reveals three configurations that have similar behavior at large times but show the effects of the settling velocity and the (negative) buoyancy term. This study enhances our understanding of incompressible flows with buoyancy effects and provides insights into the behavior of such fluid systems in a two-dimensional domain. Overall, this investigation improves our knowledge of fluid dynamics and how the concentration is transported in the direction of flow in two-dimensional domain, offering potential for optimizing processes involving incompressible fluids in similar configurations. The presented approach serves as a foundation for future studies and optimizations in various engineering applications, in particular for the case of biological reactors as the Upward Anaerobic Sludge Blanket (UASB) reactor.*

Keywords: *Boussinesq approximation, Finite Elements, Gridap, Navier-Stokes, UASB reactor.*

1. INTRODUCTION

According to Batstone et al. (2002), high rates of organic load and low production of sludge are among the many advantages of anaerobic processes. One of the main drivers for

the increased application of anaerobic processes is energy production. The biogas produced can also replace fossil fuel sources and, therefore, has a positive effect on reducing greenhouse gases. In this way, the anaerobic digestion processes for waste treatment in the future will increase drastically.

Several benefits are expected from a generalized model of anaerobic digestion like increased model application for full-scale plant design, operation, and optimisation as well as a common basis for further model development and validation studies to make outcomes more comparable and compatible (IWA, 2002). The IWA (2002) presents the ADM1, which stands for Anaerobic Digestion Model No.1, as applicable as possible to anaerobic processes. Batstone et. al. (2002) explain that the physico-chemical system refers to processes in anaerobic reactors that are not mediated by biological activity.

According to Oliveira (2022), anaerobic digestion is also used in non-conventional effluent treatment plants, such as the UASB (Upflow Anaerobic Sludge Blanket) type high-rate reactor, due to their low implementation cost, and because they have methane-rich biogas as a by-product. The performance of this type of reactor depends on the balance between flow mixing, that promotes more efficient process kinetics, and particle decantation, which is required for the conservation of the active biological community in the reactor. Hence, the optimal design of UASB reactors requires an understanding of the fluid dynamics and particulate transport, governed by the Navier-Stokes and particle transport equations.

The Navier-Stokes equations are non-linear partial differential equations, composed of two main equations: conservation of mass and conservation of momentum. In this study, a code, using the Finite Element Method, was developed and used to solve numerically the incompressible Navier-Stokes equations with the Boussinesq approximation, coupled to the particle concentration transport equation. The code uses a Cartesian mesh element-based approach and makes use of different finite element spaces such as test spaces and multifield spaces. The study parameters of this problem are the magnitude of velocity, pressure, and concentration.

The mathematical modeling for the solution of this problem was done using programming in the Julia language using the Gridap package through the Visual Studio Code software, and then the simulation results were visualized through the ParaView software version 5.11.1. According to Badia, S. & Verdugo, F. (2020), Gridap is a new Finite Element (FE) framework, exclusively written in the Julia programming language, for the numerical simulation of a wide range of mathematical models governed by partial differential equations (PDEs).

2. MATHEMATICAL FORMULATION

2.1 Strong Formulation

The Navier-Stokes equations with the Boussinesq term were adapted from Pontes, J. & Mangiavacchi, N. (2016) and Tritton (1977) and can be written in their dimensionless form, combined with the concentration transport equation, and mass conservation. The strong

formulation of the problem is, therefore, given by the following system of equations:

$$\begin{cases} \dfrac{\partial \mathbf{u}}{\partial t} + \mathbf{u} \cdot \nabla \mathbf{u} = -\nabla p + \dfrac{1}{\mathrm{Re}} \nabla^2 \mathbf{u} + \dfrac{1}{\mathrm{Fr}^2} C \mathbf{g} \\ \dfrac{\partial C}{\partial t} + \mathbf{u}_p \cdot \nabla C = \dfrac{1}{\mathrm{Re}\,\mathrm{Sc}} \nabla^2 C \\ \nabla \cdot \mathbf{u} = 0 \end{cases} \tag{1}$$

with appropriate boundary and initial conditions, as will be discussed below. In the expressions above, t represents time; $\mathbf{u}$ is the velocity vector of the fluid; $\mathbf{g}$ is a unit vector that points in the direction of gravity, that is, in the two-dimensional case, pointing in the y direction:$\mathbf{g} = [0, -1]$; p is the pressure; C is the concentration; $\mathrm{Re} = \rho U_c L_c / \mu$ is the Reynolds number; ρ is the fluid density; μ is the viscosity of the fluid, U_c is the characteristic dimensional average velocity; L_c is the dimensional characteristic length; $\mathrm{Fr} = U_c / \sqrt{g_c L_c \Delta\rho / \rho}$ is the modified (or densimetric) Froude number; g_c is the magnitude of the dimensional gravity acceleration; $\Delta\rho$ is the density variation at the inflow concentration; $\mathrm{Sc} = \mu / \rho D$ is the Schmidt number; $\mathbf{u}_p = \mathbf{u} + \mathbf{u}_s$ is the particle velocity, given by the flow velocity plus the relative settling velocity $\mathbf{u}_s$; C represents the particle concentration.

2.2 Weak Formulation

The weak formulation, associated to solve the system of PDEs (equation 1), leads to coupled non-linear systems of equations for the unknowns $\mathbf{u}$, p, and C with the time derivative written explicitly. The weights associated with velocity, pressure and concentration are, respectively, $\mathbf{v}$, q and r.

The weak boundary value formulation is based on two types of function spaces. A trial function space is composed of candidate solutions which satisfy any Dirichlet boundary condition present in the strong formulation. The weighting function space, however, is composed of arbitrary functions that are equal to zero at the boundaries where Dirichlet boundary conditions are imposed. It is required that member functions of both of these spaces, together with their respective derivatives, be square-integrable. That is, they belong to the following function spaces:

Let U, P and C be trial function spaces for the velocity $\mathbf{u}$, pressure p and particle concentration C, respectively. Such spaces are defined as follows:

$$\begin{aligned} \mathrm{U}(\Omega) &= \{\mathbf{u} \in H^1(\Omega) : \mathbf{u} = \mathbf{u}_\Gamma \text{ on } \Gamma\}, \\ \mathrm{P}(\Omega) &= \{p \in L_2(\Omega) : p = p_\Gamma \text{ on } \Gamma\}, \\ \mathrm{C}(\Omega) &= \{C \in H^1(\Omega) : C = C_\Gamma \text{ on } \Gamma\}. \end{aligned}$$

The corresponding weighting function spaces are:

$$\begin{aligned} \mathrm{V}(\Omega) &= \{\mathbf{v} \in H^1(\Omega) : \mathbf{v} = \mathbf{0} \text{ on } \Gamma\}, \\ \mathrm{Q}(\Omega) &= \{q \in L_2(\Omega) : q = 0 \text{ on } \Gamma\}, \\ \mathrm{R}(\Omega) &= \{r \in H^1(\Omega) : r = 0 \text{ on } \Gamma\}, \end{aligned}$$

where $L_2(\Omega) = \left\{ f : \int_\Omega f^2 \, d\Omega < \infty \right\}$ and $H^1(\Omega) = \left\{ f : f \in L_2, \int_\Omega \left(\frac{\partial f}{\partial x_i} \right)^2 \, d\Omega < \infty \right\}$.

Each equation, in its strong form, is then multiplied by one weighting function, and integrated over the domain Ω. The combination of all equations results in the following formulation:

$$\int_\Omega \frac{\partial \mathbf{u}}{\partial t} \cdot \mathbf{v}\, d\Omega + \int_\Omega ((\mathbf{u} \cdot \nabla \mathbf{u}) \cdot \mathbf{v} - (\nabla \mathbf{v})p + \frac{1}{\mathrm{Re}} \nabla \mathbf{u} : \nabla \mathbf{v} + \frac{1}{\mathrm{F_r}^2} \mathbf{g} \mathbf{v} C)\, d\Omega + \\ + \int_\Omega q(\nabla \cdot \mathbf{u})\, d\Omega + \int_\Omega \frac{\partial C}{\partial t} r\, d\Omega + \int_\Omega ((\mathbf{u}_p \cdot \nabla C) r + \frac{1}{\mathrm{Re\ Sc}} \nabla C \cdot \nabla r)\, d\Omega = 0 \quad (2)$$

Here, it was considered that there are no non-homogeneous Neumann boundary conditions.

3. DOMAIN DISCRETIZATION

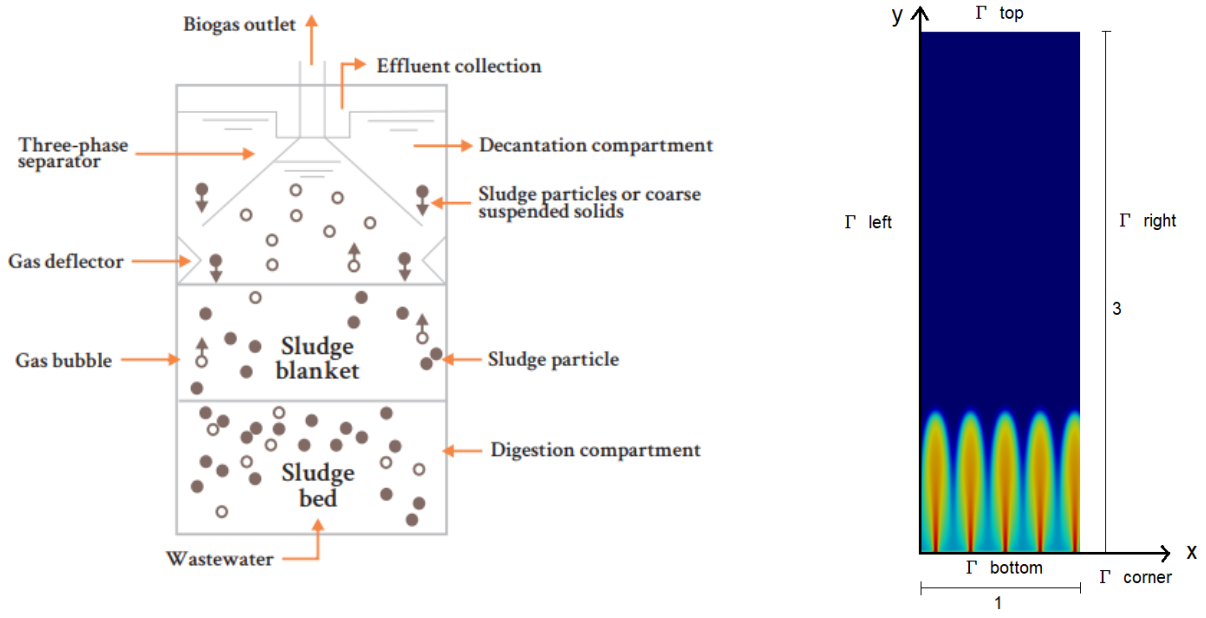


Figure 1: UASB biodigester. Left: operating scheme (Kunz, 2022). Right: model geometry and boundary conditions.

The simulation in our code involves solving a transient problem governed by the Navier-Stokes equations and the concentration transport equation. To fully define the problem, appropriate initial and boundary conditions are required. Fig. 1 shows a scheme of a UASB bioreactor as presented by Kunz (2022), and a representation of the domain and boundary conditions employed in the current computational model.

3.1 Mesh partitioning and boundary conditions

The code modeled a periodic rectangular two-dimensional (2D) domain, so we have two main directions: x, the horizontal direction, and y, the vertical direction. $L_x = 1$ represents the width of the domain, while $L_y = 3$ represents the height of the domain. Next, the mesh partitioning was carried out, that is, we divided the domain into rectangular finite elements. The partition variable indicates how the domain will be subdivided into finite elements. In this

case, the division is done in n elements in the x direction and $3n$ elements in the y direction. Proper partitioning is essential to obtain accurate and efficient results in the solution of partial differential equations. The Gridap library which can be accessed on GitHub (2023) was used to perform the spatial discretization of the mesh. It was considered a 120×360 cartesian mesh over a rectangular 1×3 non-dimensional domain.

Appropriate initial and boundary conditions are specified to complete the problem statement. The initial condition for the velocity field $\mathbf{u}$ is defined as follows:

$$\mathbf{u}^{(0)}(\Omega) = (0, 0). \tag{3}$$

This initial condition sets the initial velocity field throughout all domain Ω. The boundary conditions for the velocity field is prescribed at the bottom:

$$\mathbf{u}(\Gamma_{\text{bottom}}) = (0, V_y), \tag{4}$$

where V_y is null at the region between the inflow jets, and is equal to 10 in the jet regions.

The domain is considered periodic in the horizontal direction, hence Γ_{left} and Γ_{right} represent periodic boundaries for all the variables.

The initial condition for the concentration field C is defined as follows:

$$C^{(0)}(\Omega) = 0. \tag{5}$$

This initial condition sets the initial concentration field throughout all domain Ω.

The boundary condition for the concentration field is specified on the bottom boundary (Γ_{bottom}) as

$$C(\Gamma_{\text{bottom}}) = 1.0 \tag{6}$$

This condition enforces a prescribed concentration value of 1.0 on the bottom boundary.

The pressure field p does not have any specific initial condition. Instead, it is determined by the incompressibility constraint. The boundary condition pressure is specified on the top boundary (Γ_{top}) as

$$p(\Gamma_{\text{top}}) = 0.0 \tag{7}$$

4. NUMERICAL SCHEME

These initial and boundary conditions, along with the weak formulation and temporal integration method, fully define the transient problem solved by our code.

For the numerical approximation, we used a similar strategy to Badia, S. & Verdugo, F. (2020) for the velocities, creating a conventional vector-valued continuous Lagrangian Finite Element space. Considering T an arbitrary cell of the FE mesh $\mathcal{T}$, and $Q_k(T)$ the local polynomial interpolation function in cell T defined as the multi-variate polynomials in T of order less or equal to k in each spatial coordinate. This is the usual continuous vector-valued Lagrangian Finite Element space of order k defined on a mesh of quadrilaterals (BADIA; VERDUGO, 2020). P_{k-1} is the local polynomial interpolation function of polynomials in T of degree less or equal to $k-1$.

The space for the pressure is:

$$Q_0 = \left\{ q \in Q : \int_\Omega q \nabla \cdot \mathbf{u} \, d\Omega = 0 \right\}, \quad \text{with} \tag{8}$$

$$Q = \left\{ q \in L^2(\Omega) : q|_{\mathcal{T}} \in P_{k-1}(T) \quad \text{for all} \quad T \in \mathcal{T} \right\}. \tag{9}$$

In this work, we selected a quadratic interpolation ($k = 2$), to velocity field and concentration. A first order interpolation was used for the pressure. Functions in Q_0 are strongly constrained to have zero mean value. This is achieved in the code by removing one Degree Of Freedom (DOF) from the interpolation space Q and adding a constant to the computed pressure so that the resulting function has zero mean value.

In order to solve this nonlinear weak formulation, Equation (2), the Newton method was used. For that, is necessary to compute the Jacobian associated with the residual of the formulation. This computation is performed by automatic differentiation using the Julia NLsolve package as can be found in Libraries.io (2023).

5. RESULTS AND DISCUSSIONS

The developed model was used to study the dynamics of particulate concentration in a reactor. The main objective is to determine conditions that improve the effectiveness of the mixing provided by the bottom injection, without compromising the separation and settling characteristics at the top of the reactor.

Simulations were performed to analyze the effect of the coupling between concentration and velocity fields produced by the buoyancy term, which is modulated by the Froude number, and the magnitude of the settling velocity $\|\mathbf{u}_s\|$. The values of the parameters employed in the simulations are summarized in the Tab. 1.

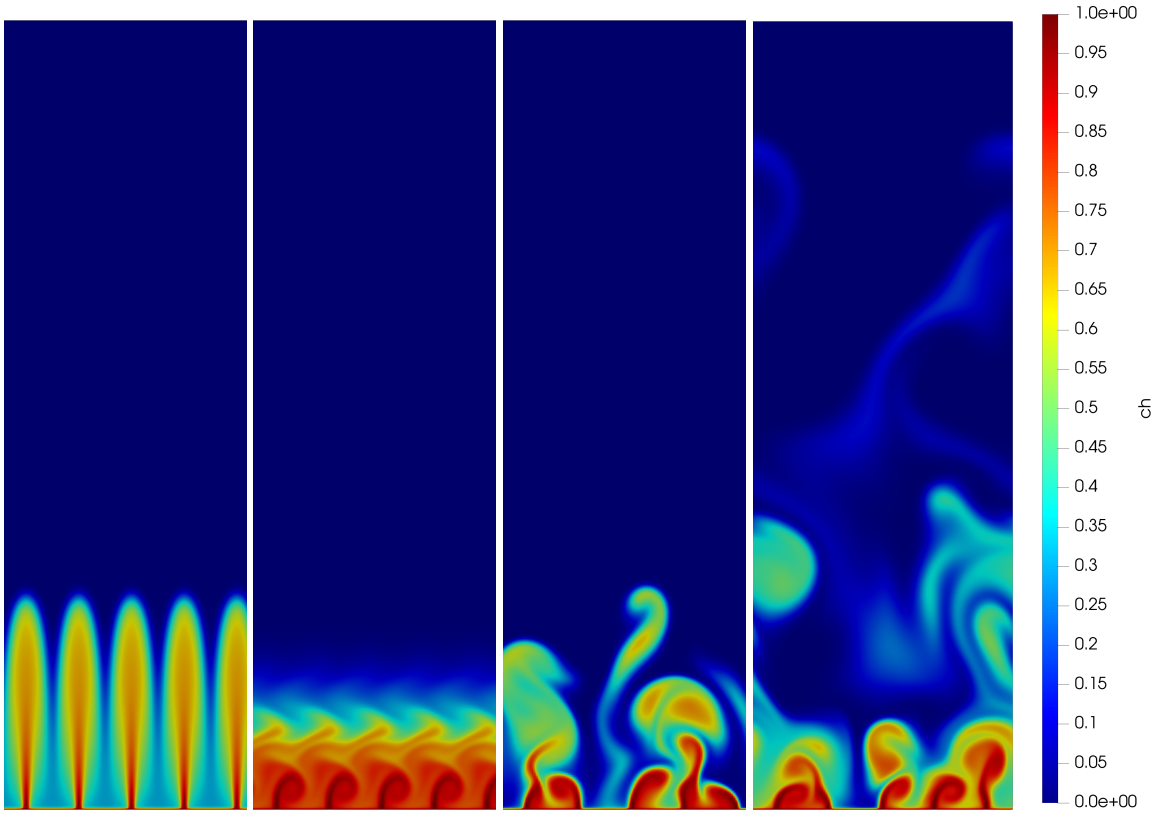
Case	Re	Fr	$\|\mathbf{u}_s\|$	Sc
A	300	0.01	1.1	1
B	300	0.1	1.1	1
C	300	0.01	1.5	1

Table 1: Simulation parameters.

The simulations represent the motion of the fluid in a tank stirred by the bottom injection through five equally spaced injection points. The evolution of the flow can be effectively visualized by the particle concentration distribution during the simulation time. The concentration fields at four representative times for case B are shown in Fig. 2.

The flow develops in three stages. At the first stage ($t = 1$, Fig. 2-a), the jets develop without interaction, and the flow reaches a quasi-stationary solution. This first regime is initially disrupted by periodic perturbations that synchronize the movement of the jets ($t = 3.5$, Fig. 2-b). These perturbations are periodic both in time and space. During this regime, the concentration boundary layer is seen to shrink and remain more attached to the bottom.

This regime is eventually disrupted by a secondary instability that breaks the periodic symmetry of the flow ($t = 4.7$, Fig. 2-c). The jets are then seen to interact in pairs and triplets that alternate in a nonperiodic fashion ($t = 7$, Fig. 2-d). Even though the particulate jets are visibly diverted by gravity effects, there are some lumps of particles with reduced concentration that reach higher regions of the reactor. However, the top of the reactor is not reached by any important amount of particles, thus essentially no particles escape from the reactor.



a) $t = 1.0$ b) $t = 3.5$ c) $t = 4.7$ d) $t = 7.0$

Figure 2: Time evolution of the concentration field for case B, at various times. The flow is seen to evolve from a quase-stationary regime, to a periodic regime and eventually reaches a chaotic regime

The velocity and vorticity fields obtained in configuration case B are shown in Fig. 3. The flow is unsteady and the figure represents a snapshot at $t = 7$, at a time when the flow has undergone a turbulent transition and is characterized by a typically chaotic regime.

A comparison of the effect of the simulation parameters is provided by Fig. 4. It can be seen that the three configurations have similar behavior at large times. Configuration A shows a more uniform distribution of concentration up to about 1/3 of the height of the reactor, while for cases B and C, the particulate remains more attached to the bottom. Case C, corresponding to a larger magnitude of the settling velocity, also shows a stronger stratification effect, as expected.

From the perspective of the reactor performance, configuration A seems the more adequate, providing a relatively more uniform distribution at the lower 1/3 of the reactor, however without compromising the separation of particulate at the top of the reactor.

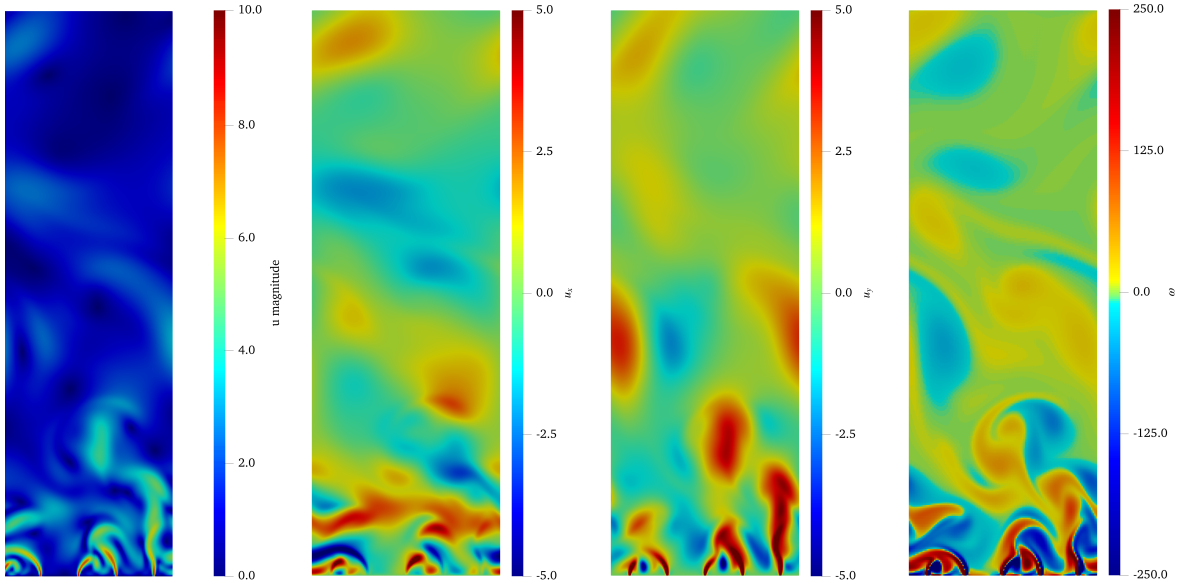


Figure 3: Velocity magnitude, u_x, u_y, and ω, for case A at $t = 7$.

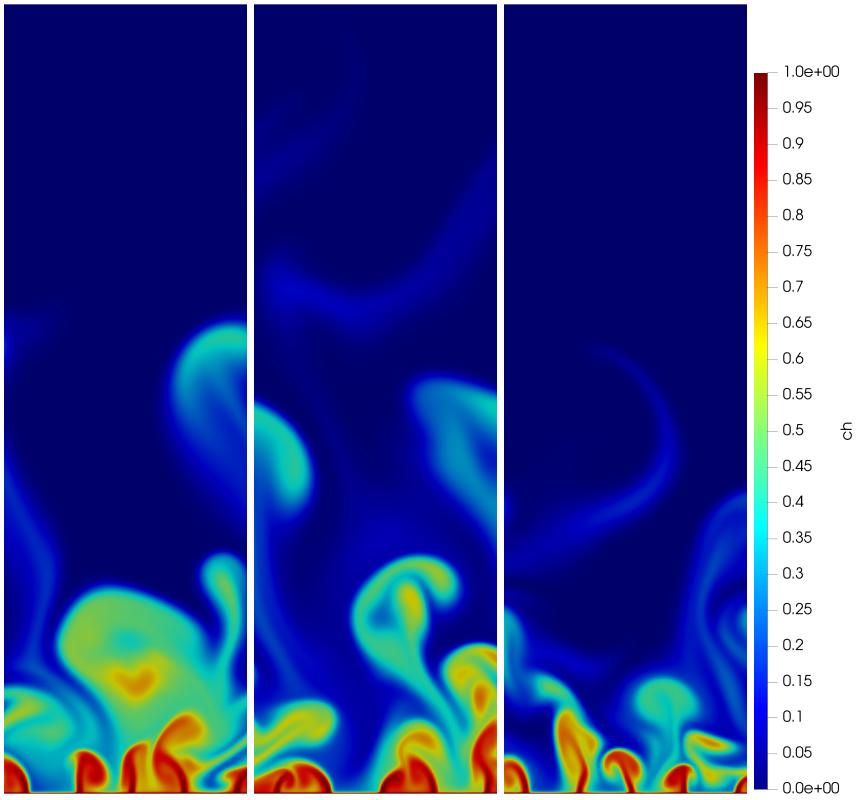


Figure 4: Particulate concentration for cases A, B and C at time $t = 7$.

6. CONCLUSIONS

In this study, we present the direct numerical simulation of a low-Reynolds incompressible turbulent particulate flow in a two-dimensional domain using the finite element method, so as to further comprehend the effects of buoyancy on the flow. The results reveal that the flow behavior is significantly impacted by particulate concentration gradients, leading to more complex and turbulent flow patterns. More importantly, it illustrates the delicate balance between turbulence and stratification phenomena necessary for the optimal performance of decantation reactors.

The analysis of the weak formulation of the incompressible flow problem highlights the importance of the chosen finite element spaces for numerical accuracy and stability. Employing higher-order interpolation spaces allows for a more precise approximation of velocity and pressure fields. The validity and effectiveness of the numerical method are confirmed by comparing the results with known analytical solutions.

The results suggest that tangible improvements to processes involving both mixing and stratification can be attained by careful consideration of operational and design parameters, which directly benefit from CFD simulations. Given the turbulent flow patterns observed, a more realistic study in three-dimensional space would provide further insight into the relationship between the aforementioned parameters and the fluid flow and particulate transport behaviour.

This study contributes to the understanding and modeling of incompressible flows with buoyancy effects, which is relevant for various practical applications in engineering and physical sciences. Overall, this work provides a solid foundation for future research in incompressible turbulent particulate flow simulation and suggests the potential for further enhancements to extend the model to more complex and realistic cases.

Acknowledgements

This study was financed in part by the Coordenação de Aperfeiçoamento de Pessoal de Nível Superior – Brasil (CAPES) – Finance Code 001. The authors aknowledge support by CNPq, FINEP, FAPERJ and UERJ.

REFERENCES

Batstone, D. J., Keller, J., Angelidaki, I., Kalyuzhnyi, S. V., Pavlostathis, S. G., Rozzi, A., ... & Vavilin, V. A. (2002), *"The IWA anaerobic digestion model no 1 (ADM1)*". *Water schimience and technology*, 45(10), 65-73.

IWA (2002), *"Iwa task group for mathematical modelling of anaerobic digestion processes. Anaerobic Digestion Model No 1 (ADM1): schimientific and Technical Report No. 13.*", First Edition, 2002.

Oliveira, G.G. (2022), "*Simuladores de Processos Anaerobios*", Dissertação de Mestrado, Faculdade de Engenharia/UERJ, Rio de Janeiro.

Rincon, M.A. and IShih, L.I.U. (2013), *"INTRODUÇÃO AO MÉTODO DE ELEMENTOS FINITOS – Computação e Análise em Equações Diferenciais Parciais*", Rio de Janeiro: Instituto de Matemática, Universidade Federal do Rio de Janeiro, Rio de Janeiro.

Tritton, D. J. (1977), *"Physical Fluid Dynamics. The Modern University in Physics Series*", Van Nostrand Reinhold Co., New York.

Kunz, et al. (2020), *Fundamentals of anaerobic digestion, biogas purification, use and treatment of digestate*, Embrapa Swine & Poultry.

Badia, S., & Verdugo, F. (2020), *Gridap: An extensible finite element toolbox in julia*, Journal of Open Source Software,5(52), 2520.

Verdugo, F., & Badia, S. (2022), *The software design of Gridap: a finite element package based on the Julia JIT compiler*, Computer Physics Communications, 276, 108341.

Verdugo, F., & Badia, S. (2019), *A user-guide to Gridap–grid-based approximation of partial differential equations in Julia.*, Journal of Open arXiv preprint arXiv:1910.01412.
Pontes, J., & Mangiavacchi, N. (2016), *Fenômenos de Transferência com Aplicações às Ciências Físicas e à Engenharia–Volume 1: Fundamentos.*, Sociedade Brasileira de Matemática (SBM).
GitHub (2023), *Repositório do GitHub.* URL: https://github.com
Libraries.io (2023), *NLsolve on Libraries.io.* URL: https://libraries.io/julia/NLsolve